Magnetic and crystal-field properties of the magnetic superconductor DyNi$_2$B$_2$C from ^{161}Dy Mössbauer spectroscopy

J. P. Sanchez

Département de Recherche Fondamentale sur la Matière Condensée, Commissariat à l'Energie Atomique/Grenoble,
17 rue des Martyrs, 38054 Grenoble Cedex 9, France

P. Vulliet

Département de Recherche Fondamentale sur la Matière Condensée, Commissariat à l'Energie Atomique/Grenoble,
17 rue des Martyrs, 38054 Grenoble Cedex 9, France
and Université J. Fourier, Grenoble, France

C. Godart

CNRS, UPR-209, Place A. Briand, 92195 Meudon Cedex, France

L. C. Gupta, Z. Hossain, and R. Nagarajan

Tata Institute of Fundamental Research, Bombay 400 005, India

(Received 18 April 1996)

We have utilized the ^{161}Dy Mössbauer effect to investigate the magnetic properties and the nature of the ground state of the DyNi$_2$B$_2$C quaternary magnetic superconductor ($T_N \sim 11$ K, $T_c \sim 6$ K). Detailed analysis of the spectra suggests that the magnetic transition is of first order and the Dy moments of 9.8μ_B at saturation are confined in the basal plane. Isomer shift in this material (~ 0.5 mm/s) is significantly less than that observed in metallic Dy which implies charge transfer from 6s orbitals of Dy onto the strongly bonded C atoms. The second-order B_2^0 crystal-field parameter is positive and estimated to amount to about 2 K. The ground-state crystal-field doublet is composed primarily of the $|\pm 1/2\rangle$ component of the $J=15/2$ free ion term. Higher-order crystal-field terms should be included in the exchange crystal-field Hamiltonian for a detailed account of the experimental results. [S0163-1829(96)00937-X]

I. INTRODUCTION

The superconductivity research has gained a new momentum after the finding of superconductivity in the multiphase quaternary Y-Ni-B-C system.[1,2] Superconductivity was found in the single phase materials RNi$_2$B$_2$C with superconducting transition temperature varying from 8.5 to 16.5 K for $R =$ Ho, Er, Tm, Y, Lu.[3] The structure of these materials has been found to be the body-centred-tetragonal structure of a ''filled'' variant of the ThCr$_2$Si$_2$-type (space group $I4/mmm$).[4] Superconductivity has been found to coexist with antiferromagnetic order for the heavy rare earths Tm, Er, Ho for temperatures below $T_N = 1.5$, 5.85, and 6.0 K, respectively.[5–10] Coexistence was not established conclusively in earlier investigated polycrystalline DyNi$_2$B$_2$C sample.[3,10] However, subsequent works on either single-crystalline[11,12] or polycrystalline samples[13–16] clearly showed onset of superconductivity at $T_c \sim 6.5$ K, while antiferromagnetic order sets in at $T_N \sim 11$ K. The ways in which magnetism and superconductivity coexist is one of the main topics of interest in this field of research. A great amount of work has been devoted to the study of the magnetic and superconducting properties of the RNi$_2$B$_2$C series. It is to be pointed out that DyNi$_2$B$_2$C is the only member of the RNi$_2$B$_2$C series to exhibit $T_c < T_N$ and only in two other materials [Er$_2$Fe$_3$Si$_5$ (Ref. 17) and Tb$_2$Mo$_3$Si$_4$ (Ref. 18)] T_c has been found to be less than T_N. Therefore, it is of importance to investigate in detail the properties of DyNi$_2$B$_2$C.

The present study reports on detailed ^{161}Dy Mössbauer measurements of the hyperfine field (H_{hf}) and of the quadrupole coupling constant (e^2qQ) at the Dy site in DyNi$_2$B$_2$C. Both hyperfine parameters are sensitive to the nature of the electronic state of the Dy^{3+} ions, as fashioned by the magnetic interactions and the crystalline electric field (CEF) produced by the neighboring ions in the lattice. The hyperfine interaction data, when supplemented by bulk magnetization data and neutron-diffraction results, are expected to provide information about the strength of the molecular field and the crystal-field parameters (B_n^m).

DyNi$_2$B$_2$C has been extensively studied by bulk magnetization[11,14] and neutron diffraction.[19–21] It was found that DyNi$_2$B$_2$C is a simple collinear antiferromagnet below $T_N \sim 10.3$ K. The Dy moments are aligned ferromagnetically in each rare-earth-carbon layer perpendicular to the c axis with the layers themselves coupled antiferromagnetically.[19–21] The magnetization data reveal a strong magnetic anisotropy which confines the Dy moments in the basal plane.[11] This indicates that crystal-field effects play an essential role. Field-induced magnetic transitions were observed around 1 and 1.15 T in a polycrystalline sample and a saturated Dy magnetic moment of 8.9μ_B is achieved in 5 T field at 2 K.[14,16] Finally, the analysis of the magnetic entropy associated with the magnetic ordering indicates a quartet or
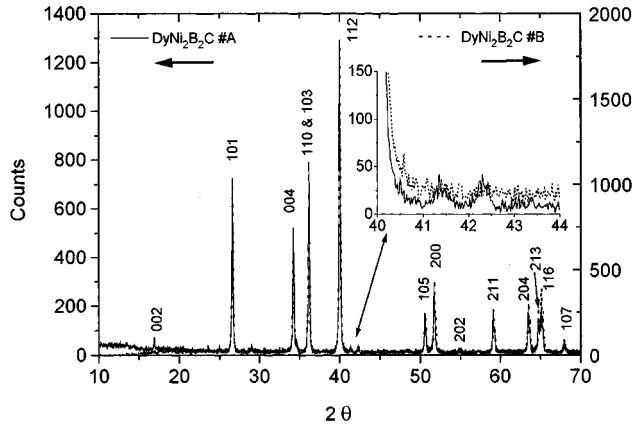
FIG. 1. RT powder x-ray-diffraction patterns of polycrystalline DyNi$_2$B$_2$C samples (A and B). The inset shows the impurity lines observed at $2\theta=41.4$ and $42.3°$ in sample A.

two low-lying CEF doublets.[14,16]

The paper has been organized in the following way. In Sec. II we give a brief account of the samples preparation and characterization. In Sec. III we present the ^{161}Dy hyperfine interaction measurements. In Sec. IV we discuss our results in the frame of an exchange and crystal-field Hamiltonian and present our conclusions concerning the crystal-field parameters acting at the R site in the RNi$_2$B$_2$C series.

II. SAMPLES PREPARATION AND CHARACTERIZATION

The two DyNi$_2$B$_2$C samples A and B used in this study were prepared by arc melting, under purified argon atmosphere, and subsequent annealing as described in a previous paper.[22] Room-temperature x-ray-diffraction measurements on the polycrystalline materials were performed using either a Jeol or a Philips automatic diffractometer (Fig. 1). They showed that both samples crystallize in the expected LuNi$_2$B$_2$C-type structure.[4] The lattice constants evaluated from a least-squares fit of the x-ray line positions were found to be similar within experimental errors for sample A [$a=3.532(1)$ and $c=10.482(3)$ Å] and sample B [$a=3.531(1)$, $c=10.488(3)$ Å] and in good agreement with other published values.[11,14] Some additional weak diffraction lines were observed in sample A at $2\theta=23.5$, 25.0, 29.0, 41.4, and 42.3°. Except the peaks at 29.0 and 41.4° they may be attributed to a DyB$_2$C$_2$ impurity phase[23] whose level should not exceed 2.5% of the main phase.

The onset of magnetic ordering and superconductivity in our samples was established using a standard four-probe technique for the resistance measurements and a standard mutual inductance method for the ac-susceptibility measurements. A distinct drop of the resistance observed in both samples around 11 K is attributed to the reduction in the magnetic scattering due to the onset of magnetic order below T_N. The subsequent drop at about 6 K is related to the occurrence of superconductivity (Fig. 2). While a zero resistance is already observed at 3.8 K in sample A, R extrapolates to zero only at 2.4 K for sample B. The temperature dependence of the ac susceptibility (χ_{ac}) of samples A and B is shown in the right inset of Fig. 2. Similar to the R measurements, two anomalies are observed in both samples. The
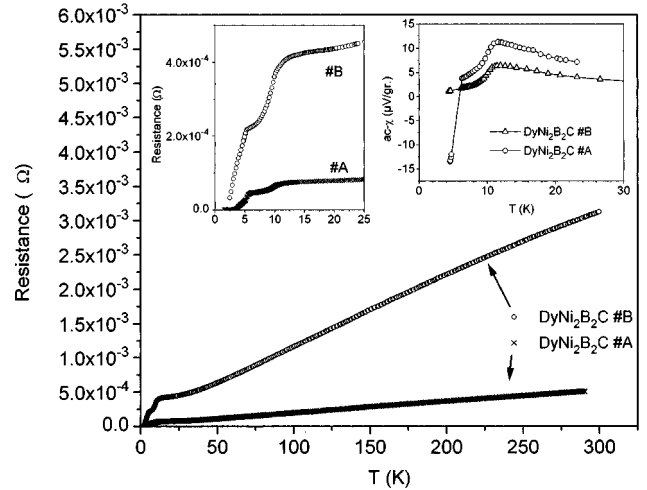
FIG. 2. Resistance *versus* temperature curves for DyNi$_2$B$_2$C samples (A and B). Left inset is an expanded view showing that resistance vanishes at different temperatures in the two samples. Right inset shows ac susceptibility (normalized to the masses) *versus* temperature for the two samples and emphasizes that magnetic ordering temperature does not change.

peak at ~ 11 K is associated with the magnetic ordering of the Dy moments. The drop in susceptibility observed for sample A below 6 K corresponds to a diamagnetic signal from the superconducting phase. Although χ_{ac}, in sample B, decreases too at ~ 6 K it does not change its sign, i.e., no diamagnetic signal is seen. It is concluded from resistance and χ_{ac} measurements that coexistence of magnetism and superconductivity is clearly established in sample A. The presence of impurity phases in sample A [particularly the low concentration of the ferromagnetic DyB$_2$C$_2$ (Ref. 24)] is not detrimental to the observation of bulk superconductivity. In fact the initial C content of the sample has been shown to be a crucial parameter in determining superconducting properties,[13] however B and C being close light elements, no experimental measurements of their concentrations were performed on our samples or reported in the literature. On the other hand, other causes like residual strains can lead to an extrinsic suppression of T_c.[11]

III. ^{161}Dy HYPERFINE INTERACTION MEASUREMENTS

A. Experimental procedure

The ^{161}Dy Mössbauer measurements (5/2→5/2, 25.7 keV) were performed using a sinusoïdal drive motion of a neutron irradiated ^{160}Gd$_{0.5}$^{162}Dy$_{0.5}$F$_3$ source kept at room temperature. The source was prepared from 50 mg of material in a flux of 10^{14} n cm^{-2} s^{-1} during 5 days. Mössbauer spectra of the absorbers were taken at different temperatures between 1.6 and 300 K. Absorber thicknesses of about 30 mg Dy/cm^2 were used. The γ rays were detected with an intrinsic Ge detector. The velocity scale was calibrated using the NMR data of metallic Dy. The effective-field magnetic spectra were directly least-squares computer fitted to their hyperfine parameters by constraining the relative absorption energies
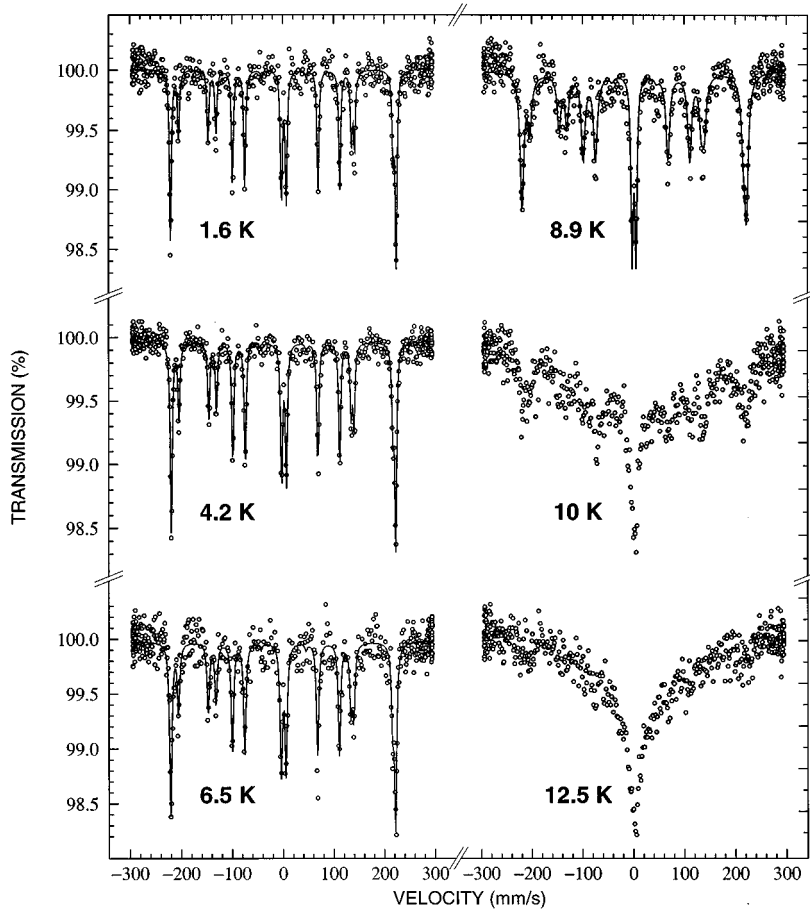
FIG. 3. ^{161}Dy Mössbauer spectra of DyNi$_2$B$_2$C (sample B) at different temperatures. The 1.6, 4.2, and 6.5 K spectra were fitted with a "static" hyperfine Hamiltonian. The 8.9 K spectrum was fitted with a two-level exchange split relaxation model (see text).

and intensities of the Lorentzian lines to the theoretical values. Some of the spectra were analyzed using spin-relaxation models described in Sec. III B.

B. Experimental results

Figure 3 shows spectra taken at temperatures between 1.6 and 12.5 K for sample B. Although similar spectral shapes were observed for sample A one notices that the linewidth is, however, slightly broader at low temperature (1.6–4.2 K) for sample B. This is most clearly seen in Fig. 4 in the 4.2 K spectra recorded on a smaller velocity scale (the doublet in Fig. 4 is the central part of the magnetically split spectrum fully shown in Fig. 3) which, in addition, allow an accurate determination of the isomer shift. The isomer shift relative to the source [0.46(2) mm/s and 0.53(3) mm/s for samples A and B, respectively] is significantly smaller than the one observed in metallic Dy [2.88(6) mm/s] or in DyM_2Si$_2$ intermetallics.[25] This behavior is tentatively assigned to the strong chemical bond between the rare-earth and carbon atoms[4] resulting in a charge transfer from the Dy 6s orbitals onto the C atoms. Although the difference of isomer shift between sample A and B is minute it is reasonable to attribute that difference to a smaller C content in sample B.

The 1.6–6.5 K spectra can be well analyzed by a static hyperfine Hamiltonian with a unique set of hyperfine parameters with electric-field-gradient axis parallel to the hyperfine field, i.e., to the Dy magnetization axis. The values of hyperfine fields and quadrupole interaction strengths, measured at

various temperatures, are given in Table I. The severe line broadening observed at 8.9 K (Fig. 3) indicates that the spectral shape is influenced by relaxation effects. It can be accounted for by using an exchange-split two-level relaxation model with a single relaxation time.[26] It should, however, be emphasized that this model is rather phenomenological; a more realistic model should take into account all transitions involving the populated exchange-split crystal-field levels. Indeed, according to specific-heat data[14,16] the ground state is a quartet or consists of two close doublets. The 10 K spectrum (Fig. 3) can no longer be reproduced by using the two-level relaxation model. The spectral shape actually appears to be a superposition of a relaxation broadened magnetic split subspectrum and of a spectrum similar to those observed just above T_N (i.e., where the magnetic hyperfine structure is collapsed as in the 12.5 K spectrum). This behavior as well as the observation of an hyperfine field which is T independent at least up to 10 K, indicate that the magnetic transition is first order with a narrow ($\leqslant 2$ K) temperature range where magnetically ordered and paramagnetic domains coexist. This is consistent with the neutron-diffraction data which show that the intensity of the magnetic Bragg peaks is saturated at ~ 8 K.[19–21] It is worth mentioning that the relaxation rate $\Omega \approx 10^9$ Hz does not reach the fast relaxation limit ($\Omega \approx 10^{11}$ Hz) even at temperatures far above T_N where standard quadrupolar spectra are not observed. Figure 5 shows the Mössbauer spectrum recorded at RT. Relaxation effects are still clearly visible. The RT data can be straight-
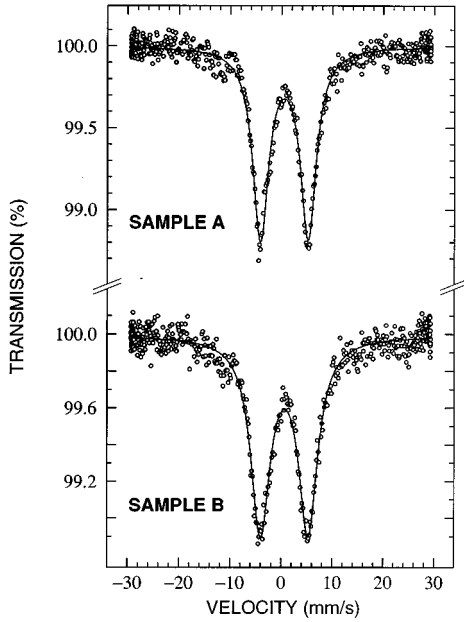
FIG. 4. 4.2 K Mössbauer spectra of DyNi$_2$B$_2$C samples (A and B) recorded on a smaller velocity scale showing the occurrence of broader linewidth for sample B [W=3.8(1) mm/s vs 4.6(2) mm/s].

forwardly reproduce by using the Wegener relaxation model[27] with a quadrupole coupling constant $|e^2qQ|$ amounting to 33(2) mm/s.

IV. DISCUSSION

A. Hyperfine field and quadrupolar interaction

The magnetic hyperfine field acting on rare-earth nuclei is commonly described as a sum of several contributions.[28] The most important one (H_{4f}) comes from the $4f$ electrons. Apart from the $4f$ contribution there will be a component (H_s) arising from the s electrons.

The effective quadrupole coupling constant e^2qQ consists of an electronic ($4f$) and a lattice (lat) contribution. The possible contribution of conduction electrons is included in the lattice term. The lattice electric-field-gradient (efg) contribution (of axial symmetry in our case) can be treated as a perturbation of the $4f$ component. Its projection along this component gives[29]

TABLE I. Hyperfine interaction parameters in DyNi$_2$B$_2$C at different temperatures obtained from a ''static'' hyperfine Hamiltonian and a two-level relaxation analysis.

T (K)	H_{hf} (kOe)	e^2qQ (mm/s)[a]	W (mm/s)
1.6	5 590 (20)	112.6(9)	4.4(2)
4.2	5 607 (20)	112.9(6)	4.7(2)
6.5	5 614 (30)	112.7(9)	5.6(2)
8.9	5 620(40)[b]	112(2)[b]	4.5[c]

[a]For E_γ=25.7 keV in Dy: 1 mm/s=8.5576×10^{-8} eV=20.69 MHz.
[b]From two-level relaxation model least-squares fit.
[c]Fixed value.
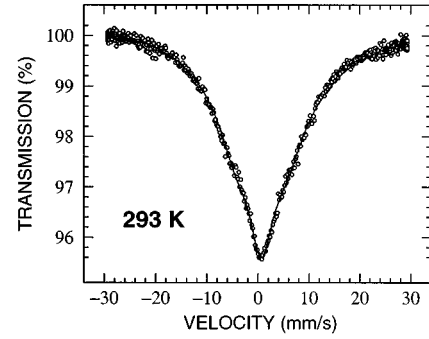
FIG. 5. RT ^{161}Dy Mössbauer spectrum of DyNi$_2$B$_2$C. The data representing a relaxation broadened quadrupolar spectrum were least-squares analyzed using the Wegener relaxation model (Ref. 27).

$$e^2qQ=e^2q_z^{4f}Q+\frac{1}{2}\,e^2q_{z'}^{lat}Q(3\cos^2\theta-1), \qquad (1)$$

where θ is the polar angle defining the orientation of the lattice efg principal axis z' with respect to the direction of the hyperfine field (or magnetic moment) taken as the z axis. In our case, the z' axis of the lattice efg is along the tetragonal c axis.

The $4f$ contribution to e^2qQ and H_{hf} give useful information concerning the electronic structure of the Dy^{3+} ions. Indeed, the 16-fold degeneracy of the ground-state multiplet ($^6H_{15/2}$) is lifted by the crystalline electric field (CEF) and the molecular field (MF) acting on the $4f$ shell. If $|\Gamma_i\rangle$ is the wave function of the ith electronic level, the $4f$ contributions to the z component of the hyperfine field and efg are proportional to $\langle\Gamma_i|\hat{J}_z|\Gamma_i\rangle$ and $\langle\Gamma_i|3\hat{J}_z^2-J(J+1)|\Gamma_i\rangle$, respectively. Thus, both hyperfine parameters are sensitive to the wave functions of the ground and excited levels.

For an S-state ion, the $4f$ contribution to H_{hf} vanishes, thus $H_{hf}\approx-279$ kOe measured in isostructural GdNi$_2$B$_2$C (Ref. 30) provides a direct evaluation of the H_{4f} contribution in DyNi$_2$B$_2$C when scaling the Gd data with the spin $S=(g_J-1)J$ factor 5/7. With this procedure H_s is evaluated to amount to -200 kOe. The small difference between the hyperfine coupling constant for Gd and Dy was not taken into account because it will at most introduce a change of roughly 10 kOe on the scaled value. From the measured magnetic hyperfine field of 5590 kOe at 1.6 K (Table I) it follows that the saturated H_{4f} in DyNi$_2$B$_2$C amounts to 5800(30) kOe. Its comparison with the free ion Dy^{3+} estimate of 5930(30) kOe (Ref. 25) allows us to evaluate $\langle J_z\rangle\approx7.33(8)$ and the saturated magnetic moment $m=9.8(1)\mu_B$ of the Dy ions.

The $4f$ contribution to e^2qQ also vanishes for a Gd^{3+} ion. This allows the ''lattice'' contribution to be calculated in the isostructural DyNi$_2$B$_2$C from the quadrupolar data of GdNi$_2$B$_2$C [eq_z=11.9×10^{21} V/m^2 (Ref. 30)]. From e^2qQ (^{155}Gd)=5.36 mm/s, measured in GdNi$_2$B$_2$C and from the known values of the ground-state quadrupole moments: Q (^{155}Gd)=1.30(2) b and Q (^{161}Dy)=2.35(16) b, the lattice contribution to the quadrupolar interaction at the ^{161}Dy nuclei was estimated to amount to 32.7(3) mm/s. This value corresponds well to the quadrupolar interaction measured at RT. This indicates that all CEF levels are populated at RT

TABLE II. Values of B_2^0, predicted CEF ground state by $B_2^0 \hat{O}_2^0$ Hamiltonian and comparison between predicted (B_2^0 model) and measured moment direction for $R\mathrm{Ni_2B_2C}$ compounds.

| | | | | Easy direction | |
	B_2^0 (K) (Mössbauer)[a]	B_2^0 (K) (susceptibility)[b] (Refs. 6 and 11)	CEF ground state	B_2^0 model	Experimental (Refs. 6, 9, and 11)
R					
Tb	3.45	>0	0	No moment	Basal plane
Dy	2.06	1.42	$\pm 1/2$	Basal plane	Basal plane
Ho	0.69	0.85	0	No moment	Basal plane
Er	−0.75	−0.02	$\pm 15/2$	c axis	Basal plane
Tm	−2.86	−1.15	± 6	c axis	c axis

[a]From Eq. (4) using the ^{155}Gd measurements in $\mathrm{GdNi_2B_2C}$ (Ref. 30).
[b]From $B_2^0 = 10(\theta_\perp - \theta_\parallel)/3(2J-1)(2J+3)$.

(i.e., the $4f$ contribution to the efg at that temperature is vanishingly small). As shown by single-crystal magnetization measurements[11] and by neutron results[19–21] the Dy moments are in the basal plane and the angle θ in Eq. (1) is equal to 90°. Therefore the electronic $4f$ contribution to the efg amounts to 128.8(9) mm/s at saturation, considering that the measured quadrupole interaction strength is 112.6 mm/s (Table I). If one takes $e^2 q^{4f} Q = 135(1)$ mm/s for the free ion Dy^{3+} value,[25] $\langle 3\hat{J}_z^2 - J(J+1)\rangle$ amounts to about 100(1.5). Furthermore if one assumes that $\langle J_z^2 \rangle \approx \langle J_z \rangle^2$ one finds $\langle J_z \rangle \approx 7.38$ in rather good agreement with the value estimated from H_{4f} (7.34).

B. Crystal and molecular fields parameters in $\mathrm{DyNi_2B_2C}$

The sequence of low-lying Dy^{3+} electronic levels in directly related to the CEF parameters B_n^m and to the molecular field (H_{mol}) through the Hamiltonian which has the following form:

$$\mathcal{H}_{\mathrm{CEF}} + \mathcal{H}_{\mathrm{MF}} = B_2^0 \hat{O}_2^0 + B_4^0 \hat{O}_4^0 + B_4^4 \hat{O}_4^4 + B_6^0 \hat{O}_6^0 + B_6^4 \hat{O}_6^4$$
$$- g_J \mu_B H_{\mathrm{mol}} \hat{J}_z , \qquad (2)$$

where the $\hat{O}_n^m$ are the Stevens operator equivalents. In the absence of molecular field, i.e., in the paramagnetic state, the degeneracy of the $^6H_{15/2}$ multiplet is partially lifted into a set of eight Kramers doublets. The general wave functions of these doublets can be written as

$$\Gamma_1 = a_1 |\pm 1/2\rangle + b_1 |\mp 7/2\rangle + c_1 |\pm 9/2\rangle, \dots, \Gamma_8 = a_8 |\pm 15/2\rangle$$
$$+ b_8 |\pm 7/2\rangle ,$$

where the coefficient a_i should be considered larger than the corresponding b_i or c_i. The latter are due to the off-diagonal terms associated with the B_4^4 and B_6^4 CEF parameters. When these parameters are very small in comparison to B_2^0, B_4^0, and B_6^0, the wave functions become pure $|\pm m\rangle$ states whose energy spacings are determined by the relative signs and magnitudes of B_2^0, B_4^0, and B_6^0.

An estimate of the B_2^0 CEF parameter can be obtained from the lattice contribution to the efg, i.e., from ^{155}Gd measurements in $\mathrm{GdNi_2B_2C}$.[30] B_2^0 is related to the Gd quadrupolar interaction $\Delta E_Q = e^2 q Q$ by the relation[31]

$$B_2^0 = \alpha_J \langle r^2 \rangle_{4f} (1 - \sigma_2) A_2^0 \qquad (3)$$

with $A_2^0 = -\Delta E_Q / 4e(1 - \gamma_\infty)Q$. The quantity A_2^0 is an universal factor applicable to all isostructural compounds of rare earths, α_J is the Stevens factor and $\langle r^2 \rangle_{4f}$ is the mean-square radius of the $4f$ wave function, varying from one rare earth to another. σ_2 is a screening coefficient estimated to amount about 0.6 for any rare-earth atom. γ_∞ is the Sternheimer antishielding factor of the efg produced by the lattice charges. $(1 - \gamma_\infty)eQ$ is evaluated to amount 1.21×10^{-6} Å^2. With this selection of atomic parameters relation (3) can be rewritten as

$$B_2^0(K) \approx -277 \alpha_J \langle r^2 \rangle_{4f} \Delta E_Q$$

and

$$A_2^0 (K \, Å^{-2}) \approx -692 \Delta E_Q , \qquad (4)$$

when $\alpha_J \langle r^2 \rangle_{4f}$ is given in Å^2 units and ΔE_Q in mm/s. The α_J and $\langle r^2 \rangle_{4f}$ factors are tabulated by Hutchings[32] and Freeman and Desclaux,[33] respectively. With $\Delta E_Q = 5.36$ mm/s,[30] one obtains from relation (4), $B_2^0 = 2.06$ K and $A_2^0 = -3710$ (K Å^{-2}) One should however keep in mind that relation (3) is only justified for ionic compounds; its usefulness for intermetallic systems has been recently questioned.[30,34] Nevertheless, Eq. (3) seems to predict correctly (except for the Er compound) the sign and magnitude of B_2^0 and consequently the easy direction of magnetisation in the $R\mathrm{Ni_2B_2C}$ series as shown in Table II.

From the magnitude of B_2^0 in $\mathrm{DyNi_2B_2C}$ it is tempting to consider that $B_2^0 \hat{O}_2^0$ is the dominant term in the CEF Hamiltonian. In such a situation Eq. (2) reduces to

$$\mathcal{H} = B_2^0 [3\hat{J}_x^2 - J(J+1)] - g_j \mu_B H_{\mathrm{mol}} \hat{J}_z ,$$

where the x axis is the crystal c axis; z represents the direction of the Dy moments in the basal plane. This Hamiltonian allows us to calculate the magnetic moment $m = g_J \mu_B \langle \Gamma_i | \hat{J}_z | \Gamma_i \rangle$ as well as the matrix element $\langle \Gamma_i | 3\hat{J}_z^2 - J(J+1) | \Gamma_i \rangle$ of the ground state as a function of the ratio $R = g_J \mu_B H_{\mathrm{mol}}/B_2^0$.[35] From $m = 9.8 \; \mu_B$ and $\langle 3\hat{J}_z^2 - J(J+1) \rangle \approx 100$ evaluated in Sec. IV A, one deduces that R amounts to about 10.[35] Thus, with B_2^0 in the range 1.4–2.1 K (Table II) the molecular field should be 155–230 kOe, a rather unrealistic high value. Indeed, $H_{\mathrm{mol}} \approx 43$ kOe evaluated from the Néel temperature using the relation $g_J \mu_B H_{\mathrm{mol}} = 3k_B T_N/(J+1)$ is significantly smaller. Although this misfit may arise, at least partially, from anisotropic ex-

change interactions as evidenced in $GdNi_2B_2C$,[36] the interplay of higher-order CEF parameters has certainly to be taken into account. It is worth recalling here that, according to specific-heat data,[14,16] the ground state is either a quartet or consits of two close doublets. The B_2^0 CEF model, on the other hand, predicts a $|\pm 1/2\rangle$ ground state with a first excited doublet at about 12 K. The shortcoming of the B_2^0 model is, however, best illustrated by the behavior of $ErNi_2B_2C$ where the Er moments are found to be in the basal plane,[6,9] while the model predicts that they should be along the c axis. The interplay of higher-order CEF parameters is most sensitive for $ErNi_2B_2C$ because B_2^0 has the smallest value among the RNi_2B_2C series (Table II). Since the magnetization of $ErNi_2B_2C$ is in the basal plane while B_2^0 is negative and small, B_4^0 and (or) B_6^0 should be positive. Furthermore, since the β_J and γ_J Stevens factors for Dy and Er have opposite and same signs, respectively it is anticipated that B_4^0 should be negative and B_6^0 positive in $DyNi_2B_2C$. At this stage it is not possible to make other predictions about the higher-order CEF parameters in $DyNi_2B_2C$. It is expected that they will be deduced in a near future through a detailed interpretation of single-crystal susceptibility and magnetization data together with specific-heat and neutron inelastic-scattering measurements in the whole RNi_2B_2C series.

V. CONCLUSIONS

Our ^{161}Dy Mössbauer effect measurements on the magnetic superconductor $DyNi_2B_2C$ indicate that the magnetic transition at $T_N \sim 11$ K is first order. The two samples that were investigated had different superconducting properties, but do not show any significant difference in the hyperfine interaction parameters. The analysis of the hyperfine field and of the quadrupole coupling constant allow us to conclude that the Dy moments of 9.8 μ_B are confined in the basal plane and that $\langle J_z^2 \rangle \approx 54.6$ at saturation. The crystal-field ground state of mainly $|\pm 1/2\rangle$ character explains the direction of magnetization as well as the observed rather fast relaxation rate of the Dy moments which results into the collapse of the magnetic hyperfine structure above T_N. Although the second-order B_2^0 CEF parameter (which is positive and amounts to about 2 K in $DyNi_2B_2C$) plays a dominant role, it will be necessary to include higher-order CEF terms to account for the observed hyperfine interaction strengths. A significant observation in our measurements is that the value of the isomer shift is closer to those in nonmetallic Dy systems. This suggests that the Dy-C layer basically is a nonconducting layer which in turn implies that superconductivity arises from Ni-B layer.

[1] Chandan Mazumdar, R. Nagarajan, C. Godart, L. C. Gupta, M. Latroche, S. K. Dhar, C. Levy-Clement, B. D. Padalia, and R. Vijayaraghavan, Solid State Commun. **87**, 413 (1993).

[2] R. Nagarajan, Chandan Mazumdar, Zakir Hossain, S. K. Dhar, K. V. Gopalakrisknan, L. C. Gupta, C. Godard, B. D. Padalia, and R. Vijayaraghavan, Phys. Rev. Lett. **72**, 274 (1994).

[3] R. J. Cava, H. Takagi, H. W. Zandbergen, J. J. Krajewski, W. F. Peck, Jr., T. Siegrist, B. Batlogg, R. B. van Dover, R. J. Felder, K. Mizuhashi, J. O. Lee, H. Eisaki, and S. Uchida, Nature (London) **367**, 252 (1994).

[4] T. Siegrist, H. W. Zandbergen, R. J. Cava, J. J. Krajewski, and W. F. Peck, Jr., Nature (London) **367**, 254 (1994).

[5] B. K. Cho, Ming Xu, P. C. Canfield, L. L. Miller, and D. C. Johnston, Phys. Rev. B **52**, 3676 (1995), and references therein.

[6] B. K. Cho, P. C. Canfield, L. L. Miller, D. C. Johnston, W. P. Beyermann, and A. Yatskar, Phys. Rev. B **52**, 3684 (1995), and references therein.

[7] P. C. Canfield, B. K. Cho, D. C. Johnston, D. K. Finnemore, and M. F. Handley, Physica C **230**, 397 (1994).

[8] M. S. Lin, J. H. Shieh, Y. B. You, W. Y. Guan, H. C. Ku, H. D. Yang, and J. C. Ho, Phys. Rev. B **52**, 1181 (1995), and references therein.

[9] S. K. Sinha, J. W. Lynn, T. E. Grigereit, Z. Hossain, L. C. Gupta, P. Nagarajan, and C. Godart, Phys. Rev. B **51**, 689 (1995).

[10] H. Eisaki, H. Takagi, R. J. Cava, B. Batlogg, J. Krajewski, W. F. Peck, Jr., K. Mizuhashi, J. O. Lee, and S. Uchida, Phys. Rev. B **50**, 647 (1994).

[11] B. K. Cho, P. C. Canfield, and D. C. Johnston, Phys. Rev. B **52**, 3844 (1995).

[12] C. V. Tomy, M. R. Lees, L. Afalfiz, G. Balakrishnan, and D. McK. Paul, Phys. Rev. B **52**, 9186 (1995).

[13] C. V. Tomy, G. Balakrishnan, and D. McK. Paul, Physica C **248**, 349 (1995).

[14] M. S. Lin, J. H. Shieh, Y. B. You, Y. Y. Hsu, J. W. Chen, S. H. Lin, Y. D. Yao, Y. Y. Chen, J. C. Ho, and H. C. Ku, Physica C **249**, 403 (1995).

[15] Z. Hossain, S. K. Dhar, R. Nagarajan, L. C. Gupta, C. Godart, and R. Vijayaraghavan, IEEE Trans. Magn. **31**, 4133 (1995).

[16] Z. Hossain, L. C. Gupta, R. Nagarajan, S. K. Dhar, C. Godart, and R. Vijayaraghavan, Physica B **223-224**, 99 (1996).

[17] S. Naguchi and K. Okuda, Physica B **194−196**, 1975 (1994).

[18] F. G. Aliev, V. V. Pryadun, S. Vieira, R. Villar, J. Paredes, A. P. Levanyuk, and V. I. Yarovets, Europhys. Lett. **25**, 143 (1994).

[19] P. Dervenagas, J. Zarestky, C. Stassis, A. I. Goldman, P. C. Canfield, and B. K. Cho, Physica B **212**, 1 (1995).

[20] J. W. Lynn, Q. Huang, A. Santoro, Z. Hossain, L. C. Gupta, R. Nagarajan, R. J. Cava, J. J. Krajewski, W. F. Peck, S. K. Sinha, and C. Godart (unpublished).

[21] J. W. Lynn, Q. Huang, S. K. Sinha, Z. Hossain, L. C. Gupta, R. Nagarajan, and C. Godart, Physica B **223-224**, 66 (1996).

[22] C. Godart, L. C. Gupta, R. Nagarajan, S. K. Dhar, H. Noel, M. Potel, Chandan Mazumdar, Zakir Hossain, C. Levy-Clement, G. Schiffmacher, B. D. Padalia, and R. Vijayaraghavan, Phys. Rev. B **51**, 489 (1995).

[23] J. Bauer and O. Bars, Acta Crystallogr. B **36**, 1540 (1980).

[24] T. Sakai, G. Adachi, and J. Shiokawa, Solid State Commun. **40**, 445 (1981).

[25] K. Tomala, J. P. Sanchez, and R. Kmiec, J. Phys. Condens. Matter **1**, 4415 (1989).

[26] H. H. Wickman, in *Mössbauer Effect Methodology*, edited by I. J. Gruverman (Plenum, New York, 1966), Vol. 2, p. 39.

[27] H. Wegener, Z. Phys. **186**, 498 (1965).

[28] M. A. H. Mc Causland and I. S. McKenzie, *Nuclear Magnetic Resonance in Rare Earth Metals* (Taylor and Francis, London, 1980).

[29] G. Amoretti, M. Bogé, J. M. Fournier, A. Blaise, and A. Woja-kowski, J. Magn. Magn. Mater. **66**, 236 (1987).

[30] F. M. Mulder, J. H. V. J. Brabers, R. Coehoorn, R. C. Thiel, K. H. J. Buschow, and F. R. de Boer, J. Alloys Compounds **217**, 118 (1995).

[31] S. Ofer, I. Nowik, and S. G. Cohen, in *Chemical Applications of Mössbauer Spectroscopy*, edited by V. I. Goldanskii and R. H. Herber (Academic, New York, 1968), p. 427.

[32] M. T. Hutchings, in *Solid State Physics: Advances in Research and Applications*, edited by F. Seitz and D. Turnbull (Academic, New York, 1964), Vol. 16, p. 227.

[33] A. J. Freeman and J. P. Desclaux, J. Magn. Magn. Mater. **12**, 11 (1979).

[34] R. Coehoorn, K. H. J. Buschow, M. W. Dirken, and R. C. Thiel, Phys. Rev. B **42**, 4645 (1990).

[35] M. Bogé, J. Chappert, A. Yaouanc, and J. M. D. Coey, Solid State Commun. **31**, 987 (1979).

[36] P. C. Canfield, B. K. Cho, and K. W. Dennis, Physica B **215**, 337 (1995).